Mapping effective connectivity between the frontal and contralateral primary motor cortex using dual-coil transcranial magnetic stimulation

Karen L. Bunday[1,2], Sonia Betti[3*], James Bonaiuto[4,5,6*], Guy A. Orban[7] and Marco Davare[2]

[1]Psychology, School of Social Sciences, University of Westminster, 115 New Cavendish Street, London, UK

[2]Sobell Department of Motor Neuroscience and Movement Disorders, Institute of Neurology, University College London, 33 Queen Square, London, UK.

[3]Università degli Studi di Padova, Padova, Italy

[4]Wellcome Trust Centre for Neuroimaging, UCL Queen Square Institute of Neurology, 12 Queen Square, London, UK

[5]Institut des Sciences Cognitives Marc Jeannerod, CNRS UMR 5229, Bron, France

[6]Université Claude Bernard Lyon I, Lyon, France

[7]Università degli Studi di Parma, Department of Medicine and Surgery, Via Volturno 39E, 43125 Parma

*Joint second authors

Corresponding Author: Karen L Bunday

Psychology, School of Social Sciences

University of Westminster

Room 6.123 (Clipstone)

115 New Cavendish Street

London

W1W 6UW

Declarations of interest: none

Abstract

Background: Cytoarchitectonic, anatomical and electrophysiological studies have divided the frontal cortex into distinct anatomical and functional subdivisions. Many of these subdivisions have functional connections with the contralateral primary motor cortex (M1); however, effective neurophysiological connectivity between these regions is not well defined in humans.

Objective: We aimed to use dual-coil transcranial magnetic stimulation (TMS) to map, with high spatial resolution, the effective connectivity between different frontal regions of the right hemisphere and contralateral M1 (cM1).

Methods: TMS was applied over the left M1 alone (test pulse) or after a conditioning pulse that was applied to different targets over the right frontal cortex, while subjects sat at rest, or during the preparation of index finger abduction or a precision grip.

Results: We found four clusters in the precentral gyrus and premotor regions, namely area 6d/FEF, area 43, area 6v, and area 44, which showed significant differential modulations of contralateral MEPs at rest compared to during preparation of index finger abduction and precision grip. Moreover, two clusters in the dorsal lateral prefrontal cortex (8C and 8Av-46-8C) showed differential modulation of contralateral MEPs during preparation of index finger abduction compared to precision grip.

Conclusion: We show a gradient of task-related connectivity whereby interactions between caudal premotor regions and cM1 differentiate between rest and movement preparation, but more rostrally, interactions between dorsolateral prefrontal regions and cM1 differentiate between preparation of different types of hand movements. These results thus demonstrate the utility of dual-coil TMS to define fine-grained sub-regions in the human frontal cortex, which are functional and causally involved in hand movements.

Key words: effectivity connectivity, TMS, primary motor cortex, movement preparation, dual-coil

Introduction

The primary motor cortex (M1) and frontal regions of the brain can be distinguished by their cyto-, myelo-, receptor-based architecture and complex array of connections between each other, and other parts of the cortex (Amunts and Zilles, 2015; Fan et al., 2016; Glasser et al., 2016; Luppino and Rizzolatti, 2000; Petrides and Pandya, 1999, 2002). Anatomical studies have demonstrated that neurons in frontal areas project to M1 both ipsilaterally (Dum and Strick, 1991, 2002; Luppino and Rizzolatti, 2000) and contralaterally, via the corpus callosum (Boussaoud et al., 2005; Fang et al., 2008; Lanz et al., 2017; Marconi et al., 2003). Information provided by these connections to M1 help shape motor commands for voluntary movements such as grasping and manipulating objects. Thus, monkey studies have revealed both anatomical and functional fine-grained subdivisions within the frontal cortex which have distinctive patterns of connectivity with the primary motor cortex. While modern techniques using magnetic resonance imaging (MRI) in humans supports this evidence [e.g.(Fan et al., 2016; Glasser et al., 2016)], effective neurophysiological connectivity of these areas is less well defined.

Subdivisions within the frontal cortex are important for the planning and execution of voluntary hand movements, namely the premotor cortex (including area 44), and the dorsolateral prefrontal cortex. Monkey and human ventral and dorsal premotor areas share similar cytoarchitectural features (Kurata, 2018; Petrides and Pandya, 1999, 2002; Petrides et al., 2012). Neuroanatomical tracing techniques in the monkey have revealed that each premotor area has a specific pattern of connections (Dum and Strick, 2002; Kurata and Tanji, 1986). Importantly, premotor and primary motor regions have homotopic and heterotopic callosal projections to the contralateral hemisphere (Boussaoud et al., 2005; Fang et al., 2008; Lanz et al., 2017; Marconi et al., 2003). Single neuron recordings in monkeys have shown that anatomically defined subregions of the premotor cortex; the dorsal premotor (PMd) area F2 is particularly involved in the planning and execution of reaching movements and the ventral premotor (PMv) area F5 encodes specific hand actions [for review;(Rizzolatti et al., 2014)]. Human studies also indicate that PMd areas are associated with preparation of different hand movements (Ariani et al., 2015; Begliomini et al., 2014; Fujiyama et al., 2016; Gallivan et al., 2011), and PMv is associated with object manipulation and grasping (Binkofski et al., 1999;

Davare et al., 2008; Ehrsson et al., 2000; Grafton, 2010; Johnson-Frey et al., 2005; Koch et al., 2010).

The dorsal lateral prefrontal cortex (DLPFC) also has cytoarchitectonically distinct regions that monkeys and humans share (Petrides and Pandya, 1999; Petrides et al., 2012). Although there are no known direct ipsilateral or contralateral connections with M1 (Boussaoud et al., 2005; Fan et al., 2016; Miller, 2000), indirect communication via PM and other frontal regions is likely (Boussaoud et al., 2005; Fan et al., 2016; Lanz et al., 2017; Marconi et al., 2003; Miller, 2000). In the monkey, prefrontal cortex neurons code for the internal representations of action goals (Miller, 1999; Wise et al., 1996). Similarly, DLPFC activity is associated with action-related decision making in humans (Bernier et al., 2012; Johnson-Frey et al., 2005; Jueptner et al., 1997; Rowe et al., 2005). Thus, it is clear that the anatomical and functional organisation in the monkey and human frontal cortex is similar.

Whereas tract-tracing and microstimulation can be used to probe anatomical and effective connectivity in the monkey brain with high spatial precision, these techniques are not appropriate for non-invasive use in humans. However, effective connectivity between frontal cortical subdivisions and M1 can be probed in the human brain using transcranial magnetic stimulation (TMS) with a conditioning-test paradigm. This involves a conditioning pulse given over the frontal cortex to assess its effect on motor evoked potentials (MEPs) elicited by a test pulse applied over either ipsilateral (Baumer et al., 2009; Civardi et al., 2001; Davare et al., 2008; Koch et al., 2007) or contralateral M1 (Baumer et al., 2006; Buch et al., 2010; Fiori et al., 2017; Koch et al., 2006; Mochizuki et al., 2004). Increases in conditioned MEPs reflect net excitatory influences of the conditioning pulse location on the test pulse site while decreases in conditioned MEPs reveal inhibitory influences. Contralateral frontal cortex - M1 effective connectivity can vary depending on the stimulated site and the performed task (Baumer et al., 2006; Buch et al., 2010; Fiori et al., 2017; Fujiyama et al., 2016; Mochizuki et al., 2004).

The connectivity of subdivisions in the monkey frontal cortex is relatively well known, and while invasive human mapping studies are starting to emerge (Avanzini et al., 2016; Avanzini et al., 2018; Fornia et al., 2018; Vigano et al., 2019), few non-invasive studies in healthy

humans have attempted to map large areas of frontal cortex - M1 effective connectivity, and fewer have done so during functional tasks (Cattaneo and Barchiesi, 2011; Civardi et al., 2001). We hypothesised that conditioning TMS pulses applied over different subdivisions of the frontal cortex would reveal differential connectivity with cM1 and that varying the condition (rest *vs.* preparation of index finger abduction or a precision grip) would allow us to define the functional properties of clusters of connectivity. To test our hypotheses, we used paired-pulse TMS to examine how conditioning pulses applied the right frontal cortex affected corticospinal excitability in the opposite M1 during different tasks.

Methods

Subjects

Nine right-handed (7 female, 2 male) volunteers aged 22-41 years [age 28±6.3 years mean±SD)] participated in experiments 1 and 2. Eight subjects participated in both experiments. All subjects were right-handed, with normal, or corrected to normal vision and gave written informed consent. None of the subjects had a history of neurological disease. They were all screened for adverse reaction to TMS using the TMS safety screen questionnaire (Keel et al., 2001). The experimental procedure was approved by the ethics committee of University College London.

Recordings

Digital conversion and timing of the TMS pulses were performed with a micro CED 1401mk2 unit (Cambridge Electronic Design, Cambridge, UK). Electromyographical (EMG) recordings were made from the first dorsal interosseous (FDI) muscle of the right hand with surface electrodes (belly-tendon montage, Ag-AgCl, 10 mm in diameter). The EMG signal was amplified 1000x, high-pass filtered at 3 Hz, sampled at 5 kHz and stored for off-line analysis (CED 1401 with spike and signal software, Cambridge Electronic Design, Cambridge, UK).

Transcranial Magnetic Stimulation

Paired-pulse TMS was applied using a Magtim 200 Bistim2 stimulator (Magstim, Whitland, UK) connected to 2 figure-of-eight coils, both produced monophasic waveforms. A standard figure-of-eight coil (9 cm outer diameter, D70) was used for delivering the test pulse over M1 (TP), whereas a custom-made coil (7 cm outer diameter, Magstim custom made) was used for the conditioning pulse (CP) over PM. The test coil was applied tangentially to the scalp with the handle pointing backwards and laterally at a 45° angle to the midline inducing a posterior-anterior (PA) current in the brain (Figure 1A). The coil was systematically moved over the scalp until the optimal "hotspot" was found, identified as the scalp location that reliably produces large motor evoked potentials in the right FDI muscle (Brasil-Neto et al., 1992). The resting motor threshold (RMT), defined as the minimum intensity that induced motor evoked potentials (MEPs) of ≥50 µV in 5 out of 10 responses (Rossini et al., 2015; Rothwell et al., 1999), was determined for the right FDI muscle [RMT = 45±9% of maximum stimulator output

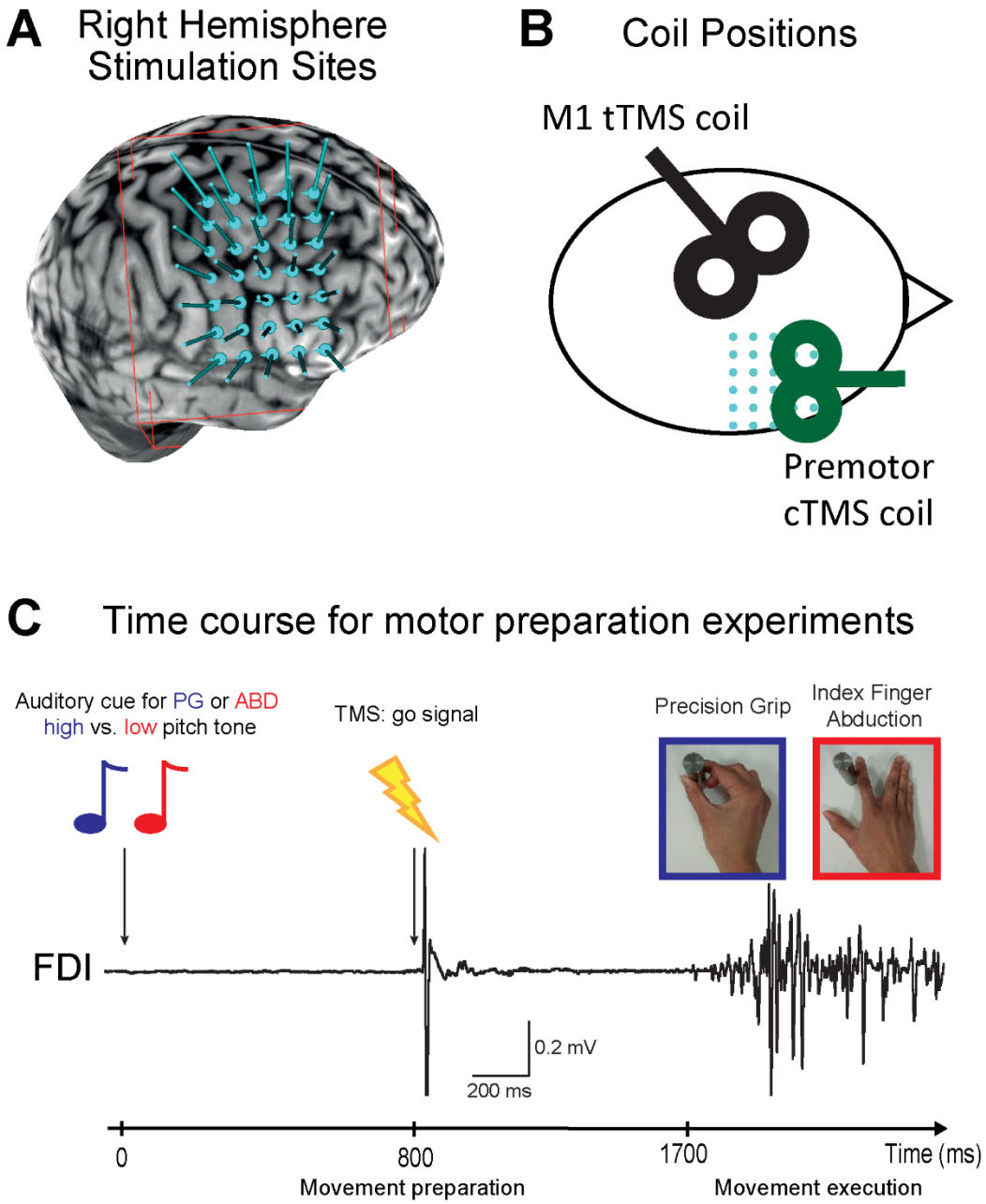

Figure 1. Experimental Setup. A. *Right hemisphere TMS stimulation targets are shown by a 5x7 grid superimposed over the right frontal cortex including the superior frontal sulcus, the central sulcus laterally and the lateral sulcus ventrally (grid distance: 10 mm). Conditioning TMS coil position was tracked online for precise stimulation over each target.* ***B.*** *Coil positions for test and conditioning TMS coils. The test TMS coil was applied tangentially to the scalp over the index finger M1 hotspot with the handle pointing backwards and laterally at a 45° angle to the midline inducing a posterior-anterior (PA) current in the brain. The conditioning TMS coil was applied to the right frontal cortex grid targets with the handle pointing forward with an anterior to posterior (AP) induced current.* ***C.*** *Time course for motor preparations experiments. An auditory cue signalled to the subject whether to perform index finger abduction or precision grip (high pitch or low pitch, respectively). TMS was triggered 800 ms after the auditory cue and constituted the "go" signal. Subjects subsequently either grasped a cylindrical object between their finger and thumb or abducted the index finger against the object.*

(MSO)]. The intensity of the TP [53±8% (mean±SD)] of maximum stimulator output (MSO)] was set to evoke an MEP of approximately 1 mV peak-to-peak amplitude in the relaxed right FDI muscle (unconditioned MEP amplitude = 1.8±0.7 mV). The conditioning pulse was delivered to the right hemisphere with the handle pointing forward with an anterior to posterior (AP) induced current (Figure 1A). The CP was set at 120% (54±12% of MSO) of the rMT (44±9% of MSO) measured with the conditioning TMS coil. The inter-stimulus interval (ISI) between the CP and TP was 8 ms (Baumer et al., 2006; Buch et al., 2010; Neubert et al., 2010; Ni et al., 2009).

The right hemisphere coil locations were determined using an MRI-aligned frameless stereotaxic neuronavigation system (Brainsight, Rogue Research). The Brainsight software 2.2.14 (Rogue Research, Montreal, Canada) was used to reconstruct a three-dimensional image of both the grey matter and the scalp surfaces. A rectangular grid (range: 26-36 targets per grid) was superimposed over the individual's right hemisphere brain surface using the anatomical MRI. The left border of the grid was aligned to the central sulcus laterally, the top border to the superior frontal sulcus rostrally, the bottom border to the lateral sulcus rostrally. The grid extended 5-6 grid points rostrally to include the precentral gyrus, middle frontal gyrus, the inferior frontal gyrus including the pars opercularis and pars triangularis. Thus, the grid included area 4, 6d, 6v, 43, FEF, 55b, 8Av, 8C, 46, p9-46v, 44, 45, (Glasser et al, 2016; Figure 1A; Suppl. Fig 1). The distance between each grid point was 10 mm, and the grid was curved to fit the individual's brain surface. The conditioning TMS coil was tracked online for precise stimulation of the grid targets; CPs were delivered to each grid point in a randomised order (Brainsight grid point randomisation).

Experimental Procedure

Experiment 1

The first experiment aimed to test the effects of conditioning TMS applied over the right hemisphere on the amplitude of MEPs recorded from the right FDI muscle, elicited by TMS applied over the left motor cortex, at rest. Participants were comfortably seated in a chair with their hands relaxed on a pillow while TMS pulses were delivered. They were instructed to keep their eyes open and to keep both hands completely relaxed. For each grid point, five conditioned and two unconditioned MEPs were acquired in random order and repeated

twice. A total of ten conditioned and four unconditioned MEPs were acquired for each grid point. Therefore, the total number of MEP ranged from 364-504.

Experiment 2

The second experiment aimed to test the effects of conditioning TMS applied over the right hemisphere on the amplitude of MEPs recorded from the right FDI muscle, elicited by TMS applied over the left motor cortex, during movement preparation. Here participants were seated comfortably in a chair with their left hand, and arm relaxed, while the right-hand voluntary contracted the FDI by index finger abduction (Prep-ABD) or grasped a solid metal cylindrical object between the index finger and thumb (precision grip; Prep-PG). An auditory cue signalled to the subject whether to perform index finger abduction or precision grip (high pitch or low pitch, respectively). The meaning of the auditory cue (low pitch/high pitch) was countered balanced between subjects. TMS was triggered 800 ms after the auditory cue and also served as the GO signal. Thus, TMS was applied during the movement preparation period (Figure 1B). Subjects were instructed to make the movement at their own pace on hearing the TMS click and to relax in between the trials. At each grid point, five conditioned and two unconditioned MEPs were acquired for preparation of index finger abduction (Prep-ABD) and precision grip (Prep-PG) in a randomised order. Due to the length of the experiment, this procedure was repeated twice in two separate sessions. Thus, over two sessions, a total of ten conditioned and four unconditioned MEPs were collected for each grid point and each movement condition. Therefore, the total number of MEPs ranged from 364-504 per session.

Data analysis

The peak-to-peak amplitudes of conditioned and unconditioned MEPs were measured for experiment 1 and 2. Conditioned MEPs were normalised and expressed as a ratio (conditioned MEP/unconditioned MEP). The unconditioned MEP was calculated by a moving average of six unconditioned MEPs (two MEPs from the current grid point + two from the previously acquired grid point + two from the next grid point) rather than to a global average of all unconditioned MEPs from the whole session. For the first and last grid points of a block, the current and next two points and the current and previous two points were used, respectively. This moving averaged unconditioned MEP allowed us to take into account small fluctuations in corticospinal excitability throughout the experimental session (2.5-3 hours).

MEPs were excluded from analysis if they were preceded by a background EMG activity greater than the resting baseline mean+2SD over a 100 ms window. In addition, for each grid point, trials in which the target error (i.e. the distance between the actual TMS stimulation point and the grid point location on the cortical surface) was 3 SD above the mean (~ > 3 mm) were discarded (Total trials excluded: Expt. 1: 2.95±1.73%; Expt. 2: 2.74±191%). For the movement experiments, RMS EMG activity during the movement was calculated in a fixed window (100 ms) starting 100 ms after the TMS artefact. A paired t-test and repeated measures ANOVAs were used to analyse background EMG pre and post TMS.

MEP maps were coregistered to each subject's MRI volume, and then 3D interpolated using SPM 12 (Functional Imaging Laboratory, Institute of Neurology, UCL, London, UK) by smoothing them with a Gaussian filter (8mm FWHM) and rescaling the smoothed maps to match the range of normalised MEP values. Each participant's cortical surface structure was reconstructed from the MRI volumes using FreeSurfer (Dale et al., 1999). The interpolated MEP maps were then projected onto the individual cortical surfaces and mapped to the FreeSurfer "fsaverage" average brain surface using the inbuilt FreeSurfer function mri_vol2surf. This mapping was completed via spherical coregistration of the surface topographies (Fischl et al., 1999), which compensates for individual anatomical differences by coregistering individual gyri and sulci.

Regions of interest (ROIs) were created by performing a one-way ANOVA on condition (rest, ABD, PG) at each vertex in the fsaverage template surface and identifying clusters with a significant main effect of condition ($p<0.05$) and including at least 55 vertices (region of approximately 80 mm in diameter). This resulted in six ROIs (Table 1 for coordinates), which were then subjected to planned comparisons between conditions (rest, Prep-ABD, Prep-PG). The centroid of each cluster was identified, and the region labelled by relating it to subdivisions of the cortex based on the Human Connectome Project brain atlas (Glasser et al., 2016), which takes into consideration existing architectonic maps of the frontal cortex (Amiez and Petrides, 2009; Amunts et al., 2010; Amunts et al., 1999; Geyer, 2004; Ongur et al., 2003; Petrides and Pandya, 1999). The anatomical subdivisions and centroids for each cluster are shown in Supplementary Figure S1.

An additional analysis was performed to show that there was significant connectivity between right frontal regions and left M1, that is, contralateral unconditioned MEPs were significantly modulated by conditioning TMS pulses. Here, we looked for any overlap between individual T-test maps for rest, Prep-ADB and Prep-PG (Fig. S2) and the map generated by the one-way ANOVA (Fig. 3). T-test maps were created by performing a one-sample T-test at each vertex of the fsaverage template surface for each condition separately (see Supplementary Materials; Fig. S3). Overlap maps and ROI clusters were created, which showed vertices that had both significant F and t-values ($p<0.05$) and included at least 55 vertices.

Results

A single TMS pulse was applied to the left motor cortical representation of the FDI muscle either alone or after a conditioning pulse was applied to the right frontal cortex, while subjects were sat at rest or just before an index finger abduction or precision grip. Normalised MEPs (conditioned MEP/unconditioned MEP) at each grid point over the right frontal cortex were used to create a motor map of physiological interactions between the right frontal cortex and cM1 during each condition (Fig. 2). Figure 3 shows the one-way ANOVA F-value motor maps where significant vertices showed a main effect of condition, thresholded at $p<0.05$. Thus, the F-value map reveals significant vertices where connectivity is different across conditions. The results revealed six clusters; planned comparisons revealed the four clusters in lateral and ventral premotor regions showed significant differences between rest and Prep-ABD, while two clusters showed additional significant differences between rest and Prep-ABD and Prep-PG. Finally, two clusters in the DLPFC showed differential effects between Prep-ABD and Prep-PG.

Note, that in experiment 1, background mean rectified EMG prior to TMS was similar across test and conditioning TMS conditions ($t_{(7)}=1.30$, $p=0.23$). In experiment 2, pre-TMS RMS EMG activity was similar across both sessions ($F_{(1,7)} = 0.11$, $p=0.75$) and task ($F_{(1,7)} = 0.02$, $p=0.88$). Similarly, post RMS EMG activity during the movement was similar across sessions ($F_{(1,7)} = 0.00$, $p=0.99$) and task ($F_{(1,7)} = 4.97$, $p=0.06$). Thus, background EMG both before and

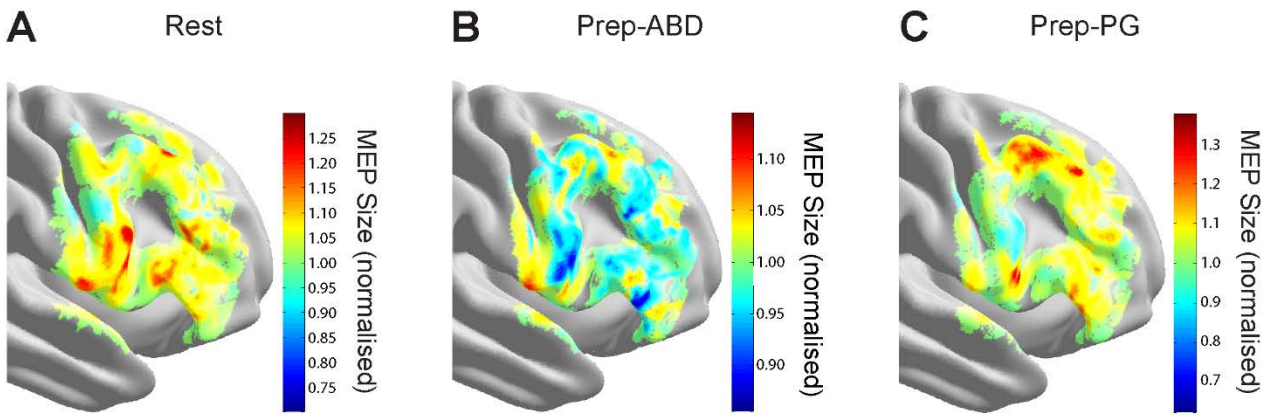

Figure 2. Normalised conditioned MEP motor maps. *TMS was applied to the left motor cortex alone, or before a conditioning pulse applied over a target over the right frontal cortex. Interpolated motor maps were created using the normalised conditioned MEPs recorded from the FDI muscle at rest (A) or during preparation of index finger abduction (Prep-ABD; B) or precision grip (Prep-PG; C) and superimposed on the freesurfer average brain. Areas shaded yellow to red represent regions where conditioned MEPs were facilitated compared to unconditioned MEPs. Areas shaded green to blue represent regions where conditioned MEPs were inhibited compared to unconditioned MEPs. Note that in ventral BA6 the motor map switches from facilitation to inhibition and back to facilitation during rest, Prep-ABD and Prep-PG, respectively. Similarly, A44V/45 switches from facilitation to inhibition and back to facilitation during rest, Prep-ABD and Prep-PG, respectively.*

after TMS did not influence the MEP results.

Premotor Regions of the Frontal Cortex

Area 6d/Frontal Eye Fields (Area 6d/FEF)

This cluster consisted of 105 significant vertices and was found in the caudolateral precentral gyrus (Fig. 3 B, C; Table 1). According to Glasser et al. (2016), the cluster centroid was found in the area 6d/FEF (Fig. S1). However, others have argued that this region is found more anteriorly and in the depth of the junction between the dorsal precentral gyrus and superior frontal sulcus (Jastorff et al., 2016). Our cluster was found on the bank of the dorsal precentral gyrus near the putative boundary between dorsal and ventral PM (Tomassini et al., 2007), since it is slightly more dorsal it has been defined as the ventral part of PMd (Avanzini et al., 2016; Avanzini et al., 2018; Fan et al., 2016; Tomassini et al., 2007), and therefore labelled Area 6d/FEF. Contralateral MEPs in this cluster were significantly facilitated by right

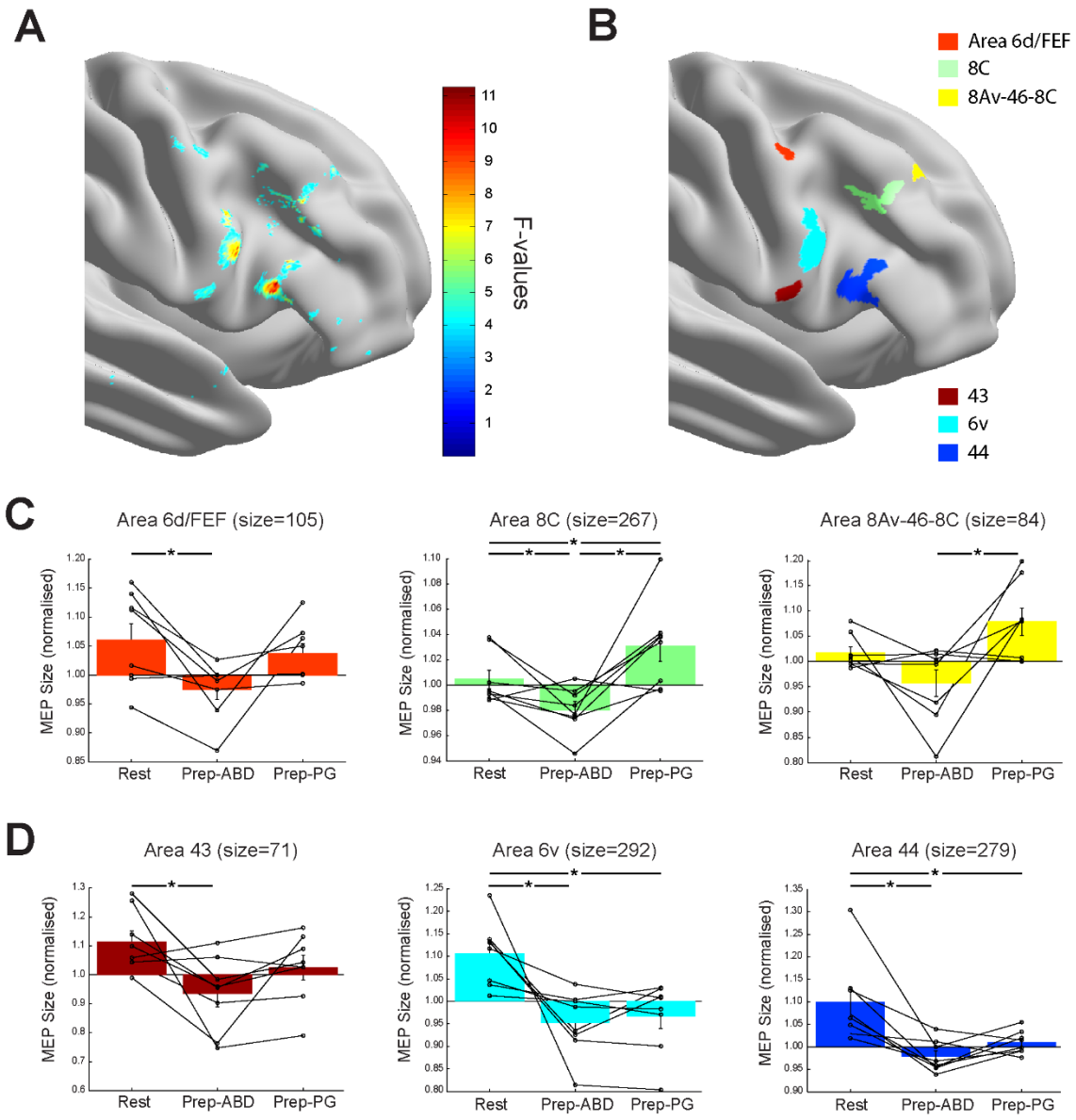

Figure 3. One-way ANOVA thresholded motor maps. A. *One-way ANOVA F-value map where F-values were thresholded at p<0.05 creating clusters in different regions of the frontal cortex. Clusters consisted of at least 55 significant vertices. Colour scale represents F-values, where blue represents low F-values and red represents high F-values.* ***B.*** *Significant main effect clusters found in the frontal cortex. Each cluster colour represents a different region and corresponds to bar graphs in C and D.* ***C & D.*** *Bar graphs showing the group (n=8) normalised MEP size during rest, Prep-ABD and Prep-PG. The abscissa shows the condition and the ordinate shows the normalised conditioned MEP size as a ratio of the unconditioned MEP. Individual subject data points are also shown (open circles). Each graphs corresponds to a region shown in B and titles show the area and number of vertices within the cluster. Error bars indicated standard error (SE). *p<0.05.*

conditioning TMS pulses at rest compared to Prep-ABD ($t_{(7)}$=3.27, p=0.014; Fig. 3B, C). No other comparison was significant (p>0.05; Fig. 3B, C). The F and t-value overlap maps revealed small clusters were MEPs were significantly facilitated at rest (p<0.05; Fig. 4A, D; Table 2), but showed a significant inhibitory change during Prep-ABD (p>0.05; Fig. 4B, E). However, the number of vertices that contributed to these clusters were below threshold (Fig. 4. B, E). A larger cluster in this region showed significant facilitation during Prep-PG (p<0.05; Fig. 4 C, F; Table 4).

Area 43

This cluster consisted of 71 significant vertices in the most ventrolateral part of the precentral gyrus and was labelled area 43 (Fig. 3 B, D; Table 1). However, the cluster centroid was found in the dorsal part of area 43 at the board of area 4 and overlapped into the face region in this area (Fig. S1). Similar to area 6d/FEF, this cluster showed a significant difference in conditioned MEPs at rest compared to Prep-ABD ($t_{(7)}$=2.86, p=0.024), but no other comparison was significant (p>0.05; Fig. 3D). The F and t-value overlap maps revealed that at rest contralateral MEPs were significantly facilitated (p<0.05), but no significantly active clusters were found for Prep-ABD and Prep-PG (p<0.05; Fig. 4; Table 2, 3, 4).

Area 6v

The largest cluster of significantly active vertices included 292 vertices and was one of three found in the ventral precentral gyrus (Table 1; Fig. 3B, D), with a cluster centroid in ventral area 6 (6v; Fig. S1). Within this cluster, conditioned MEPs at rest were significantly facilitated compared to Prep-ABD ($t_{(7)}$=3.20, p=0.015) and Prep-PG ($t_{(7)}$=2.90, p=0.023; Fig. 3B, D), while index finger abduction and precision grip conditioned MEPs showed similar effects ($t_{(7)}$=-0.83, p=0.432). The F and t-value overlap map showed that conditioned MEPs were significantly facilitated at rest (p<0.05; Fig. 4 A, D; Table 2), but a below-threshold cluster showed vertices where MEPs were significantly inhibited during Prep-ABD (p<0.05; Fig. 4 B, D). Finally, MEPs were significantly inhibited during Prep-PG (p<0.05; Fig. 4 C, F; Table 4).

Area 44

The second-largest cluster of significantly active vertices (279 vertices; Fig. 3B, D; Table 1) was found in the inferior frontal gyrus (IFG), specifically the pars opercularis. Its centroid

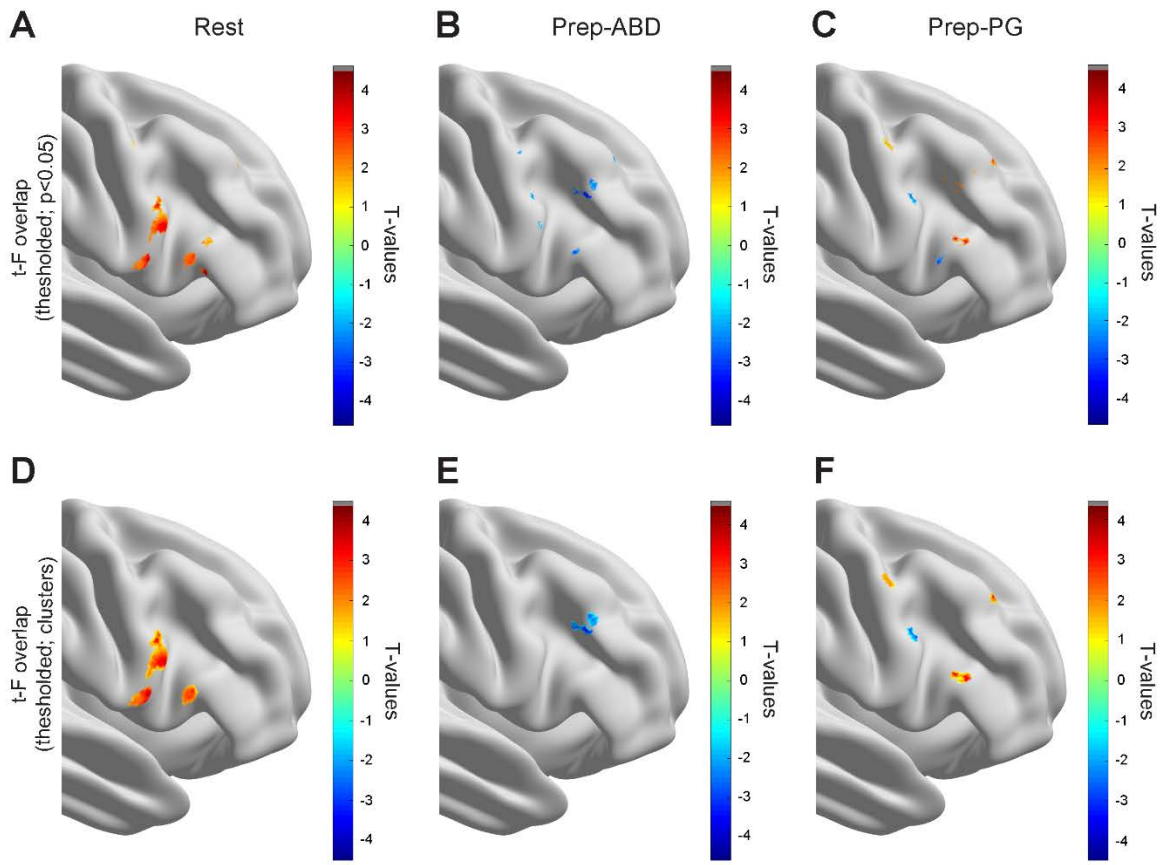

Figure 4. T-test thresholded motor maps. *T-value motor maps during rest (A), Prep-ABD (B) and Prep-PG (C), where T-values were thresholded at p<0.05 creating sub-clusters in the frontal cortex regions identified by the ANOVA motor maps. Colour scale represents T-values; where blue represents inhibition of the contralateral MEPs after conditioning right hemisphere TMS and red represents facilitation of the contralateral MEPs after conditioning right hemisphere TMS.*

was found within area 44 (Fig. S1). Like area 6v, conditioned MEPs at rest were significantly facilitated compared to prep-ABD ($t_{(7)}$=3.87, p=0.006) and prep-PG ($t_{(7)}$=3.43, p=0.011; Fig. 3B, D). Conversely, this cluster revealed a trend towards a significant difference between Prep-ABD and Prep-PG conditioned MEPs ($t_{(7)}$=-2.16, p=0.068). The F and t-value overlap clusters in this region showed that conditioned MEPs were significantly facilitated at rest (p<0.05; Fig. 4 A, D; Table 2), but only a small number of vertices showed significant inhibition during Prep-ABD (p<0.05; Fig. 4 B, E). During Prep-PG results differentiated depending on the region (Fig. 4 C,F; Table 4), that is, in the ventral part of area 44 conditioned MEPs were significantly inhibited (p<0.05; Fig. 4C), but in the dorsal part of area 44 conditioned MEPs were facilitated (p<0.05; Fig. 4C). These opposing effects likely resulted in a cancellation effect shown in the

one-way ANOVA results where area 44 showed no change in MEP size (Fig. 3D). However, only the larger facilitatory cluster survived the threshold of active vertices (Fig. 4F).

Overall, significant clusters in these predominantly premotor regions showed that conditioned MEPs were differentially modulated from rest to movement, but there was no distinction between what movement was to be performed (i.e. index finger abduction or precision grip). Further analysis revealed interactions between premotor areas and cM1 at rest are facilitatory, while only small un-thresholded clusters showed inhibition during Prep-ABD, and a mixture of inhibition and facilitation was observed in thresholded clusters during Prep-PG. The T-test maps created by performing a one-sample T-test at each vertex for each condition separately support these findings (see Supplementary materials; Fig. S3).

Dorsolateral Prefrontal Cortex (DLPFC)

Area 8C

The third-largest cluster of significantly active vertices included 267 vertices and was one of two clusters found in the middle frontal gyrus (Fig. 3B, C; Table 1). Its cluster centroid was found in the area 8C (Fig. S1). Within this cluster, conditioned MEPs were facilitated during prep-PG compared to conditioned MEPs during Prep-ABD ($t_{(7)}$=-3.74, p=0.007) and rest ($t_{(7)}$=-3.38, p=0.012; Fig. 3B, C). Differential modulation of conditioned MEPs was also found between rest and Prep-ABD ($t_{(7)}$=2.61, p=0.035; Fig. 3B, C). The F and t-value overlap maps in this region showed no significantly active vertices at rest (p>0.05; Fig. 4 A, D), but conditioned MEPs were inhibited in a significant cluster of vertices during Prep-ABD (p<0.05; Fig. 4 B, E; Table 3). A small un-thresholded cluster of significant vertices showed that conditioned MEPs were facilitated during Prep-PG (p<0.05; Fig.4 C).

Area 8Av-46-8C

A similar pattern of effects was found in a second smaller significant cluster of 84 vertices in a more rostral and dorsal region of the middle frontal gyrus (Fig. 3B, C; Table 1). Its centroid was defined as area 8Av bordered with area 46 and 8C and thus overlapped with these regions (Fig. S1). However, here only conditioned MEPs during Prep-PG were significantly facilitated compared to Prep-ABD ($t_{(7)}$=-2.67, p=0.032). Clusters in F and t-value overlap maps showed

no significantly active vertices at rest ($p>0.05$; Fig. 4A, D), while a negligible un-thresholded cluster of vertices showed significant inhibition of contralateral MEPs during Prep-ABD ($p<0.05$; Fig. 4 C). However, a thresholded cluster of significant vertices showed that MEPs were facilitated during Prep-PG ($p<0.05$; Fig. 4 C, F; Table 4).

Overall, significant clusters found in the DLPFC showed a different pattern of effects compared to the premotor regions. Here, conditioned MEPs were differentially modulated when preparing for the two different types of movement. Further analysis showed that interactions between DLPFC and contralateral M1 had a tendency to be inhibitory during Prep-ABD and switched to facilitation during Prep-PG. The T-test maps created by performing a one-sample T-test at each vertex for each condition separately support these findings (see Supplementary materials; Fig. S3).

Discussion

Our study used dual-coil TMS to examine interactions between the right frontal cortex and cM1. Based on their different effective connectivity profiles, we identified six frontal subdivisions that showed task-dependent differential modulation of corticospinal excitability. Specifically, two clusters found on the precentral gyrus (area 6d/FEF and area 43) showed a net facilitatory influence on left M1 MEPs during rest compared to index finger abduction. Two clusters found in premotor area 6v and 44 showed a net facilitatory influence on left M1 MEPs during rest compared to preparation of index finger abduction and precision grip. Finally, two clusters found in the dorsolateral prefrontal cortex, namely area 8C and 8Av-46-8C, showed a net facilitatory effect on contralateral MEPs during precision grip compared to index finger abduction. These results were confirmed by an additional analysis which showed that, at rest, premotor areas have a net facilitatory influence on cM1, while during preparation of index finger abduction, DLPFC shows had a net inhibitory effect on cM1. During preparation of precision grip, DLPFC's influence on cM1 switched to facilitation, while premotor areas exhibited a mixture of both inhibitory (area 6v) and facilitatory (area 6d/FEF, 44) interactions. Ultimately, our results show a gradient of task-related interactions wherein the posterior frontal cortex premotor regions interact with M1 by differentiating between

rest and preparing to move, but DLPFC regions differentiate between preparing different types of hand movement. Overall, these results demonstrate, for the first time non-invasively in humans, the nature of neurophysiological interactions (i.e. inhibition *vs.* facilitation) between multiple frontal subdivisions and cM1 and how these interactions change depending on the movement context.

Premotor regions

The results revealed two clusters on the precentral gyrus (area 6d/FEF and area 43) that showed differential modulation of net cM1 output when comparing rest to preparation of simple index finger abduction. In area 6d/FEF, there was a tendency for a facilitatory effect at rest, which switched to inhibition during prep-ABD, these effects were only shown in a small number of vertices, whereas a larger cluster of vertices showed a switch back to facilitation during prep-PG. We argue this cluster occupies the ventral part of PMd (Avanzini et al., 2016; Avanzini et al., 2018; Fan et al., 2016; Tomassini et al., 2007) and not FEF (Jastorff et al., 2016), especially since there is no evidence of connections between FEF and M1 (Huerta et al., 1987; Dum and Strick, 2002). Thus, differential interactions between this region and cM1 from rest to preparing to move might seem less surprising since PMd is involved in the preparation of upper limb movement (Ariani et al., 2015; Baumer et al., 2006; Begliomini et al., 2007; Begliomini et al., 2014; Gallivan et al., 2011; Rizzolatti et al., 2014). Specifically, in humans, the right and left PMd regions are crucial in the role of monitoring finger configuration during the planning and execution of hand movements (Begliomini et al., 2007; Begliomini et al., 2014). In the monkey, neurons in PMd are also responsible for movement planning and execution, where the arm is represented in the ventral region (Crammond and Kalaska, 2000; Rizzolatti et al., 2014; Wise et al., 1997). Specifically, neurons in this region convey information necessary to reach and grasp an object during the delay period before a GO signal (Wise et al., 1997). Thus, ventral PMd is likely to respond differently to rest and preparing to move as in our study.

Few TMS studies have tested this lateral premotor region for connectivity; though stimulation to medial dorsal premotor areas have a largely inhibitory influence on ipsilateral M1 at rest (Mochizuki et al., 2004; Ni et al., 2009), stimulation of a more lateral premotor site resulted

in much less inhibition or little effect at rest (Mochizuki et al., 2004). In our study, the contralateral connectivity was facilitatory but similarly less substantial at rest. However, differential connectivity was shown between rest and preparation to move. Although other TMS studies have several methodological differences compared to the current study, including stimulation location, they nonetheless have demonstrated task-dependent differential contralateral connectivity between dorsal premotor areas and cM1 (Baumer et al., 2006; Koch et al., 2006; O'Shea et al., 2007).

The second of the two clusters on the precentral gyrus that showed a differential influence on cM1 in rest compared to preparation of index finger abduction was found in area 43 but overlapped into the face region of area 4 and possibly 6v. Unlike area 6d/FEF, the differential effects in this cluster are driven mainly by a stronger facilitatory influence on cM1 at rest, since additional analysis did not reveal significant changes in MEPs compared to baseline responses during preparation of finger abduction or precision grip. Curiously, area 43 is associated with jaw and orofacial functioning, such as food intake, swallowing, speech arresting (Iwata et al., 1985; Job et al., 2011; Pallud et al., 2018; Toogood et al., 2017), although it has also been associated with vibrotactile sensation (McGlone et al., 2002). Similarly, ventral area 4 is associated with facial muscles, the tongue and larynx and functions such as chewing and swallowing (Fan et al., 2016; Glasser et al., 2016). More recently, stimulation to the trigeminal nerve has revealed response from neurons in a similar region to our cluster (Avanzini et al., 2018). It not entirely clear why connectivity in this region is present given our tasks; however, the facilitatory influence on cM1 only occurred during rest and this effect is similar to premotor regions located nearby. Since it is possible that the areal borders in this region are more gradual than sharp (Amunts and Zilles, 2015), this region could show similar connectivity.

Our results showed that there were two clusters of significant vertices within ventral PM regions (6v and 44). Here, we found a differential modulation of net cM1 output when comparing rest to preparation of index finger abduction and precision grip. Further analysis revealed that there was a significant facilitatory influence on the cM1 at rest compared to baseline. However, the switch towards inhibition during preparation of index finger abduction overall was not substantial. A more complex interaction is present during preparation of

precision grip; these regions showed different effects where area 6v showed a net inhibitory effect while area 44 showed a net facilitatory effect on cM1 compared to baseline. Within area 44 itself, there is evidence of a mixture of interactions showing that more dorsal regions show facilitatory effects whereas ventral parts tend to be more inhibitory, thus suggesting this region has complex interactions with cM1 when preparing a precision grip.

A limited number of TMS studies have examined PMv connectivity with cM1 at rest, although some evidence suggests that the influence of PMv on cM1 can be inhibitory (Fiori et al., 2017). However, the longer ISIs used in this study (e.g. 40, 150 ms) are likely to involve other cortical and subcortical networks (Fiori et al., 2017). During movement preparation, facilitatory effects of PMv on cM1 have been demonstrated (Buch et al., 2010), although the direction of these effects can be both timing and task-dependent (Buch et al., 2010; Neubert et al., 2010). Despite a similar region to our 6v being stimulated, our results contrast those of Buch et al. (2010) who revealed a facilitatory influence of PMv on cM1 during movement preparation. However, methodological differences could explain this discrepancy since TMS was delivered much earlier after the movement cue in the Buch et al. (2010) study and they also used a lower stimulation intensity (110% of RMT). Nonetheless, our and Buch et al. (2010) results might suggest that the influence of PMv on the cM1 changes during the preparation period before movement execution, is intensity-dependent, and changes depending on the type of movement to be made.

PMv forms part of the dorsolateral grasping circuit (Grafton, 2010; Grol et al., 2007; Davare, et al., 2011). In the monkey, the ventral premotor cortex likely consists of areas F4 and F5 (Rizzolatti et al., 2014) and the human PMv corresponds at least partially to F5. Neurons in these areas code for a variety of grasping actions (Rizzolatti et al., 2014), but also the goal and temporal aspects of the action (Jeannerod et al., 1995). The current study shows similar effects for the preparation of the two movement tasks in these regions (6v and 44), demonstrating that TMS given at 800 ms after the auditory cue was able to reveal encoding of movement preparation, but this encoding was unable to discriminate between the types of hand action. Nonetheless, it is interesting that clusters in area 44 show a differential influence on cM1 during preparation of precision grip, suggesting that recruitment in these closely situated regions have opposite net outputs which might reflect differences in its functional organisation.

Imaging studies show that PMv regions similar to the current study are involved in object manipulation (Binkofski et al., 1999; Ehrsson et al., 2000; Johnson-Frey et al., 2005), execution and planning of precision grasping (Grol et al., 2007). However, the latter studies only show activation in the left hemisphere and while the organisation of right and left area 6 are similar (Avanzini et al., 2018), the right and left IFG are different, where right IFG has in fact been associated with response inhibition during motor execution (Aron et al., 2014). A recent study that used whole-brain activation patterns across a large database of neuroimaging experiments showed that area 6 related to action imagination and action execution, whereas area 44 was associated with memory, encoding and spatial attention (Hartwigsen et al., 2019). However, right area 6 functionally connected to a network that includes the left area 44 and right area 44 connects to a network that includes left area 44 and 6. Thus, this provides a pathway for the effects seen in the current experiments.

Indeed, our results must be considered in relation to potential anatomical pathways. There are known ipsilateral projections from PM to M1 in the monkey (Dum and Strick, 2002; Rizzolatti et al., 2014), which also may exist in the human (Davare et al., 2008; Davare et al., 2009), so it possible that information flows first to iM1 and then to cM1 (i.e. iPM – iM1 – cM1). Alternatively, PM transcallosal projections could also transfer this information to the cM1 (Boussaoud et al., 2005; Lanz et al., 2017; Marconi et al., 2003; Rouiller et al., 1994). For instance, Rouiller et al. (1994) found that cM1 receives approximately 50% of its inputs from the premotor cortex; these are mainly found in an area close to our area 6d/FEF region. Other studies show that there are dense homotopic and heterotopic callosal connections between the right and left dorsal and ventral PM, with sparse heterotopic connections from other motor and non-motor regions (Boussaoud et al., 2005; Lanz et al., 2017). This provides the current study with two main possible pathways for the net cM1 output, namely iPM – cM1 or iPM – cPM – cM1. Since callosal projections to cM1 from premotor regions are sparse or not present in the monkey (Rouiller et al., 1994), and are likely to be faster than our ISI might allow, we suggest that the net cM1 output in our study likely results from information being passed via the contralateral PM (i.e. iPM – cPM – cM1). Our results favour this pathway since M1 transcallosal pathways project onto local circuitry before finally connecting with cM1

corticospinal neurons at ISIs of 8 and 10 ms (Di Lazzaro et al., 1999; Lee et al., 2007; Ni et al., 2009), which is comparable to our ISI.

Dorsolateral prefrontal regions

Imaging studies have shown that the DLPFC is important in action-based decision making (Bernier et al., 2012; Johnson-Frey et al., 2005; Jueptner et al., 1997; Rowe et al., 2008). Furthermore, neural activity in this area is related to behavioural goals (Yamagata et al., 2012) and the integration of information for action planning (Hoshi and Tanji, 2004; Tanji and Hoshi, 2008). We found two active clusters in regions of the DLPFC, namely area 8C and 8Av-46-8C. These clusters revealed somewhat similar results in that stimulation of these regions showed differential modulation of cM1 net output during preparation of index finger abduction and precision grip. Further analysis showed that there was no effect at rest, but these regions had an inhibitory effect on cM1 during preparation of abduction, that changed to facilitation during preparation of precision grip. These results are fundamentally different from those of the premotor regions and perhaps illuminate the role of DLPFC choosing the correct movement to make during the preparation phase. Similar TMS studies have also shown no effect of DLPFC stimulation on cM1 at rest (Mochizuki et al., 2004; Ni et al., 2009). However, a facilitatory influence on cM1 has been demonstrated when subjects prepare to make bilateral movements (Fujiyama et al., 2016). Moreover, repetitive TMS over the lateral prefrontal cortex reduces inhibition in the opposite M1 of a non-selector effector during the planning of finger movements in a choice reaction task (Duque et al., 2012). The authors suggested this region is important for selecting the appropriate response (Duque et al., 2012).

Anatomical studies have shown that there are no known ipsilateral connections between DLPFC and M1 (Miller and Cohen, 2001). However, this does not negate the fact that stimulation of this regions can affect net M1 output (Hasan et al., 2013), possibly via PMd or other frontal regions (Lu et al., 1994; Luppino et al., 1993; Miller, 2000). A recent study showed that caudal and middle regions of area 46 ipsilaterally project to both dorsal and ventral premotor regions, as well as area 8 and FEF (Borra et al., 2019). Similarly, in the human, there are known intralobular connections between DLPFC and PMd and PMv (inferior frontal gyrus – pars triangularis; (Catani et al., 2012) that information could be passed

between before being relayed to ipsilateral M1 or cM1 (i.e. DLPFC – iPMv/iPMd – iM1 – cM1 or DLPFC – iPMv/iPMd – cPMv/cPMd – cM1). As this route is quite long and connects four separate regions, it is unlikely to be compatible with the ISI used in our study. Alternatively, information concerning action choice could be relayed from DLPFC to cPMd then to cM1, since some monkey studies show strong projections from the prefrontal cortex to cPMd (Boussaoud et al., 2005). Though other contralateral DLPFC and PM projections are somewhat sparser, the number of labelled projections are non-negligible and thus still probably functionally relevant (Lanz et al., 2017; Marconi et al., 2003). Despite the route, it is clear that stimulation of the area affects net contralateral motor output in a task-dependent manner.

Methodological considerations

Evidence reveals that there are several potential pathways in which stimulation of premotor and DLPFC regions can affect contralateral motor output. Most of these pathways involve a number of synaptic connections before arriving at corticospinal neurons. Thus an ISI of 8 ms could seem relatively short; however, it has been suggested that in other established interhemispheric interactions transcallosal projections are likely to synapse onto local circuitry before information arrives at corticospinal neurons in layer V (Di Lazzaro et al., 1999; Ferbert et al., 1992; Lee et al., 2007; Ni et al., 2009). In those subjects where small effects are seen it is possible that a longer ISI could have improved effective connectivity; however, it was not possible to test several ISIs, given our experiment already contained a large number of conditions.

Modelling research has shown that TMS predominately affects the gyral crown underneath the focal point of the coil (i.e. the centre of a figure of eight coil), but surrounding areas can also be affected depending on the gyral architecture (Opitz et al., 2013; Thielscher et al., 2011). Thus, it could be possible that neighbouring clusters are artefacts of nearby TMS depending on the surrounding gyral structure. However, since we used a thresholded cluster size and the majority of our significant clusters were centimetres away from each other, this is less likely.

In the monkey, both the dorsal and ventral premotor cortex contains corticospinal neurons that terminate in the upper and lower cervical segments (Borra et al., 2010; Dum and Strick, 1991, 2002; He et al., 1993, 1995). Conduction times taken from microstimulation of these areas show that conduction velocity is slower compared to stimulating M1 (Fornia et al., 2018; Shimazu et al., 2004). Nonetheless, conditioning TMS pulses given over the frontal cortex 8 ms before the M1 test pulse modulate the resulting MEP. Therefore changes seen in MEPs could be directly affecting spinal motoneurons before M1 TMS volleys reach them. Since we did not directly test the effects of premotor stimulation on spinal circuits, we cannot rule out this possibility. However, previous studies have shown that conditioning premotor regions affect local cortical circuitry [i.e. short-interval intracortical inhibition; (Ni et al., 2009)] suggesting that these interactions are at the cortical level.

Conclusions

Monkey research has the advantage of being able to directly test the anatomy and function of different regions of the brain (Dum and Strick, 2002; Rizzolatti et al., 2014). In the human, however, this proves to be more challenging, although not impossible (Avanzini et al., 2016; Avanzini et al., 2018; Fornia et al., 2018; Vigano et al., 2019). TMS provides a method by which causality between brain regions in healthy humans can be tested, and our results show that it is possible to use dual-coil TMS to define frontal subdivisions that are important for the control of voluntary movement and shed light on the physiological nature of their interactions with M1. Changes revealed in the net motor output provide insights into how different populations of neurons respond, and how different cortical pathways are recruited in different contexts. Interestingly, our cluster analysis further highlights four segregated inputs to M1, projecting to sectors representing: the whole arm (dorsal BA6), only hand and fingers (manipulation, ventral BA6), hand and mouth/eat (BA43) and hand and mouth/speech (BA44). Ultimately, in line with previous research, our results reveal that premotor regions code for whether to move regardless of movement type and the DLPFC codes for which movement should be made. These effects show a gradient of change, where the former differential effects (i.e. whether to move or not) are located in posterior frontal regions, and anterior regions encode for different movement goals.

Acknowledgements

This work was supported by the Biotechnology and Biological Sciences Research Council (BBSRC; Grant numbers: BB/N001370/1 and BB/J014184/1).

Table 1. One-way ANOVA: Corresponding brain anatomy, brain area (Glasser et al., 2016), active cluster size (total no. of vertices), and MNI coordinates (centroid)

Neuroanatomy	**Area**	**Cluster Size**	**X**	**Y**	**Z**
Dorsal precentral gyrus	6d/FEF	105	45.14	-2.04	48.80
Ventral precentral gyrus	6v	292	56.66	7.35	28.87
Ventral precentral gyrus	43	71	63.34	0.76	13.47
Inferior frontal gyrus - Pars opercularis	44	279	55.60	18.30	15.60
Middle prefrontal gyrus	8C	267	40.21	19.01	34.59
Middle prefrontal gyrus	8Av/46/8C	84	34.14	31.48	41.11

Table 2. Rest F/t-value overlaps: Corresponding brain anatomy, brain area (Glasser et al., 2016), active cluster size (total no. of vertices)

Neuroanatomy	**Area**	**Total Sub-Clusters Size**
Ventral precentral gyrus	6v	242
Ventral precentral gyrus	43	86
Inferior frontal gyrus - Pars opercularis	44	165

Table 3. Prep-ABD F/t-value overlaps: Corresponding brain anatomy, brain area (Glasser et al., 2016), active cluster size (total no. of vertices)

Neuroanatomy	**Area**	**Total Sub-Clusters Size**
Middle frontal gyrus	8C	151

Table 4. Prep-PG F-value/T-value overlaps: Corresponding brain anatomy, brain area (Glasser et al., 2016), active cluster size (total no. of vertices)

Neuroanatomy	Area	Total Sub-Cluster Size
Dorsal precentral gyrus	area 6d/FEF	63
Ventral precentral gyrus	6v	69
Inferior frontal gyrus - Pars opercularis	44	62
Middle prefrontal gyrus	8Av/46/8C	58

References

Amiez, C., Petrides, M., 2009. Anatomical organization of the eye fields in the human and non-human primate frontal cortex. Prog Neurobiol 89, 220-230.

Amunts, K., Lenzen, M., Friederici, A.D., Schleicher, A., Morosan, P., Palomero-Gallagher, N., Zilles, K., 2010. Broca's region: novel organizational principles and multiple receptor mapping. PLoS Biol 8.

Amunts, K., Schleicher, A., Burgel, U., Mohlberg, H., Uylings, H.B., Zilles, K., 1999. Broca's region revisited: cytoarchitecture and intersubject variability. J Comp Neurol 412, 319-341.

Amunts, K., Zilles, K., 2015. Architectonic Mapping of the Human Brain beyond Brodmann. Neuron 88, 1086-1107.

Ariani, G., Wurm, M.F., Lingnau, A., 2015. Decoding Internally and Externally Driven Movement Plans. J Neurosci 35, 14160-14171.

Aron, A.R., Robbins, T.W., Poldrack, R.A., 2014. Inhibition and the right inferior frontal cortex: one decade on. Trends Cogn Sci 18, 177-185.

Avanzini, P., Abdollahi, R.O., Sartori, I., Caruana, F., Pelliccia, V., Casaceli, G., Mai, R., Lo Russo, G., Rizzolatti, G., Orban, G.A., 2016. Four-dimensional maps of the human somatosensory system. Proc Natl Acad Sci U S A 113, E1936-1943.

Avanzini, P., Pelliccia, V., Lo Russo, G., Orban, G.A., Rizzolatti, G., 2018. Multiple time courses of somatosensory responses in human cortex. Neuroimage 169, 212-226.

Baumer, T., Bock, F., Koch, G., Lange, R., Rothwell, J.C., Siebner, H.R., Munchau, A., 2006. Magnetic stimulation of human premotor or motor cortex produces interhemispheric facilitation through distinct pathways. J Physiol 572, 857-868.

Baumer, T., Schippling, S., Kroeger, J., Zittel, S., Koch, G., Thomalla, G., Rothwell, J.C., Siebner, H.R., Orth, M., Munchau, A., 2009. Inhibitory and facilitatory connectivity from ventral premotor to primary motor cortex in healthy humans at rest--a bifocal TMS study. Clin Neurophysiol 120, 1724-1731.

Begliomini, C., Caria, A., Grodd, W., Castiello, U., 2007. Comparing natural and constrained movements: new insights into the visuomotor control of grasping. PLoS One 2, e1108.

Begliomini, C., De Sanctis, T., Marangon, M., Tarantino, V., Sartori, L., Miotto, D., Motta, R., Stramare, R., Castiello, U., 2014. An investigation of the neural circuits underlying reaching and reach-to-grasp movements: from planning to execution. Front Hum Neurosci 8, 676.

Bernier, P.M., Cieslak, M., Grafton, S.T., 2012. Effector selection precedes reach planning in the dorsal parietofrontal cortex. J Neurophysiol 108, 57-68.

Binkofski, F., Buccino, G., Posse, S., Seitz, R.J., Rizzolatti, G., Freund, H., 1999. A fronto-parietal circuit for object manipulation in man: evidence from an fMRI-study. Eur J Neurosci 11, 3276-3286.

Borra, E., Belmalih, A., Gerbella, M., Rozzi, S., Luppino, G., 2010. Projections of the hand field of the macaque ventral premotor area F5 to the brainstem and spinal cord. J Comp Neurol 518, 2570-2591.

Borra, E., Ferroni C. G., Gerbella, M., Giorgetti, V., Mangiaracina C., Rozzi, S., Luppino, G. 2019. Rostro-caudal connection heterogeneity of the dorsal part of the macaque prefrontal area 46. Cereb Cortex 29, 485-504.

Boussaoud, D., Tanne-Gariepy, J., Wannier, T., Rouiller, E.M., 2005. Callosal connections of dorsal versus ventral premotor areas in the macaque monkey: a multiple retrograde tracing study. BMC Neurosci 6, 67.

Brasil-Neto, J.P., Cohen, L.G., Panizza, M., Nilsson, J., Roth, B.J., Hallett, M., 1992. Optimal focal transcranial magnetic activation of the human motor cortex: effects of coil orientation, shape of the induced current pulse, and stimulus intensity. J Clin Neurophysiol 9, 132-136.

Buch, E.R., Mars, R.B., Boorman, E.D., Rushworth, M.F., 2010. A network centered on ventral premotor cortex exerts both facilitatory and inhibitory control over primary motor cortex during action reprogramming. J Neurosci 30, 1395-1401.

Catani, M., Dell'acqua, F., Vergani, F., Malik, F., Hodge, H., Roy, P., Valabregue, R., Thiebaut de Schotten, M., 2012. Short frontal lobe connections of the human brain. Cortex 48, 273-291.

Cattaneo, L., Barchiesi, G., 2011. Transcranial Magnetic Mapping of the Short-Latency Modulations of Corticospinal Activity from the Ipsilateral Hemisphere during Rest. Front Neural Circuits 5, 14.

Civardi, C., Cantello, R., Asselman, P., Rothwell, J.C., 2001. Transcranial magnetic stimulation can be used to test connections to primary motor areas from frontal and medial cortex in humans. Neuroimage 14, 1444-1453.

Crammond, D.J., Kalaska, J.F., 2000. Prior information in motor and premotor cortex: activity during the delay period and effect on pre-movement activity. J Neurophysiol 84, 986-1005.

Dale, A.M., Fischl, B., Sereno, M.I., 1999. Cortical surface-based analysis. I. Segmentation and surface reconstruction. Neuroimage 9, 179-194.

Davare, M., Kraskov, A., Rothwell., J.C., Lemon., R.N. Interactions between areas of the cortical grasping network. Curr Opin Neurbiol 21, 565-570.

Davare, M., Lemon, R., Olivier, E., 2008. Selective modulation of interactions between ventral premotor cortex and primary motor cortex during precision grasping in humans. J Physiol 586, 2735-2742.

Davare, M., Montague, K., Olivier, E., Rothwell, J.C., Lemon, R.N., 2009. Ventral premotor to primary motor cortical interactions during object-driven grasp in humans. Cortex 45, 1050-1057.

Di Lazzaro, V., Oliviero, A., Profice, P., Insola, A., Mazzone, P., Tonali, P., Rothwell, J.C., 1999. Direct demonstration of interhemispheric inhibition of the human motor cortex produced by transcranial magnetic stimulation. Exp Brain Res 124, 520-524.

Dum, R.P., Strick, P.L., 1991. The origin of corticospinal projections from the premotor areas in the frontal lobe. J Neurosci 11, 667-689.

Dum, R.P., Strick, P.L., 2002. Motor areas in the frontal lobe of the primate. Physiol Behav 77, 677-682.

Duque, J., Labruna, L., Verset, S., Olivier, E., Ivry, R.B., 2012. Dissociating the role of prefrontal and premotor cortices in controlling inhibitory mechanisms during motor preparation. J Neurosci 32, 806-816.

Ehrsson, H.H., Fagergren, A., Jonsson, T., Westling, G., Johansson, R.S., Forssberg, H., 2000. Cortical activity in precision- versus power-grip tasks: an fMRI study. J Neurophysiol 83, 528-536.

Fan, L., Li, H., Zhuo, J., Zhang, Y., Wang, J., Chen, L., Yang, Z., Chu, C., Xie, S., Laird, A.R., Fox, P.T., Eickhoff, S.B., Yu, C., Jiang, T., 2016. The Human Brainnetome Atlas: A New Brain Atlas Based on Connectional Architecture. Cereb Cortex 26, 3508-3526.

Fang, P.C., Stepniewska, I., Kaas, J.H., 2008. Corpus callosum connections of subdivisions of motor and premotor cortex, and frontal eye field in a prosimian primate, Otolemur garnetti. J Comp Neurol 508, 565-578.

Ferbert, A., Priori, A., Rothwell, J.C., Day, B.L., Colebatch, J.G., Marsden, C.D., 1992. Interhemispheric inhibition of the human motor cortex. J Physiol 453, 525-546.

Fiori, F., Chiappini, E., Candidi, M., Romei, V., Borgomaneri, S., Avenanti, A., 2017. Long-latency interhemispheric interactions between motor-related areas and the primary motor cortex: a dual site TMS study. Sci Rep 7, 14936.

Fischl, B., Sereno, M.I., Tootell, R.B., Dale, A.M., 1999. High-resolution intersubject averaging and a coordinate system for the cortical surface. Hum Brain Mapp 8, 272-284.

Fornia, L., Ferpozzi, V., Montagna, M., Rossi, M., Riva, M., Pessina, F., Martinelli Boneschi, F., Borroni, P., Lemon, R.N., Bello, L., Cerri, G., 2018. Functional Characterization of the Left Ventrolateral Premotor Cortex in Humans: A Direct Electrophysiological Approach. Cereb Cortex 28, 167-183.

Fujiyama, H., Van Soom, J., Rens, G., Cuypers, K., Heise, K.F., Levin, O., Swinnen, S.P., 2016. Performing two different actions simultaneously: The critical role of interhemispheric interactions during the preparation of bimanual movement. Cortex 77, 141-154.

Gallivan, J.P., McLean, D.A., Valyear, K.F., Pettypiece, C.E., Culham, J.C., 2011. Decoding action intentions from preparatory brain activity in human parieto-frontal networks. J Neurosci 31, 9599-9610.

Geyer, S., 2004. The microstructural border between the motor and the cognitive domain in the human cerebral cortex. Adv Anat Embryol Cell Biol 174, I-viii, 1-89.

Glasser, M.F., Coalson, T.S., Robinson, E.C., Hacker, C.D., Harwell, J., Yacoub, E., Ugurbil, K., Andersson, J., Beckmann, C.F., Jenkinson, M., Smith, S.M., Van Essen, D.C., 2016. A multi-modal parcellation of human cerebral cortex. Nature 536, 171-178.

Grafton, S.T., 2010. The cognitive neuroscience of prehension: recent developments. Exp Brain Res 204, 475-491.

Grol, M.J., Majdandzic, J., Stephan, K.E., Verhagen, L., Dijkerman, H.C., Bekkering, H., Verstraten, F.A., Toni, I., 2007. Parieto-frontal connectivity during visually guided grasping. J Neurosci 27, 11877-11887.

Hartwigsen, G., Neef, N.E., Camilleri, J.A., Margulies, D.S., Eickhoff, S.B., 2019. Functional Segregation of the Right Inferior Frontal Gyrus: Evidence From Coactivation-Based Parcellation. Cereb Cortex 29, 1532-1546.

Hasan, A., Galea, J.M., Casula, E.P., Falkai, P., Bestmann, S., Rothwell, J.C., 2013. Muscle and timing-specific functional connectivity between the dorsolateral prefrontal cortex and the primary motor cortex. J Cogn Neurosci 25, 558-570.

He, S.Q., Dum, R.P., Strick, P.L., 1993. Topographic organization of corticospinal projections from the frontal lobe: motor areas on the lateral surface of the hemisphere. J Neurosci 13, 952-980.

He, S.Q., Dum, R.P., Strick, P.L., 1995. Topographic organization of corticospinal projections from the frontal lobe: motor areas on the medial surface of the hemisphere. J Neurosci 15, 3284-3306.

Hoshi, E., Tanji, J., 2004. Area-selective neuronal activity in the dorsolateral prefrontal cortex for information retrieval and action planning. J Neurophysiol 91, 2707-2722.

Iwata, K., Itoga, H., Ikukawa, A., Hanashima, N., Sumino, R., 1985. Movements of the jaw and orofacial regions evoked by stimulation of two different cortical areas in cats. Brain Res 359, 332-337.

Huerta., M.F., Krubitzer, L.A., Kaas, J.H., 1987. Frontal eye field as defined by intracortical microstimulation in squirrel monkeys, owl monkeys, and macaque monkeys. II. Cortical connections. J Comp Neurol 265, 332-361.

Jastorff, J., Abdollahi, R.O., Fasano, F., Orban, G.A., 2016. Seeing biological actions in 3D: An fMRI study. Hum Brain Mapp 37, 203-219.

Jeannerod, M., Arbib, M.A., Rizzolatti, G., Sakata, H., 1995. Grasping objects: the cortical mechanisms of visuomotor transformation. Trends Neurosci 18, 314-320.

Job, A., Paucod, J.C., O'Beirne, G.A., Delon-Martin, C., 2011. Cortical representation of tympanic membrane movements due to pressure variation: an fMRI study. Hum Brain Mapp 32, 744-749.

Johnson-Frey, S.H., Newman-Norlund, R., Grafton, S.T., 2005. A distributed left hemisphere network active during planning of everyday tool use skills. Cereb Cortex 15, 681-695.

Jueptner, M., Stephan, K.M., Frith, C.D., Brooks, D.J., Frackowiak, R.S., Passingham, R.E., 1997. Anatomy of motor learning. I. Frontal cortex and attention to action. J Neurophysiol 77, 1313-1324.

Keel, J.C., Smith, M.J., Wassermann, E.M., 2001. A safety screening questionnaire for transcranial magnetic stimulation. Clin Neurophysiol 112, 720.

Koch, G., Fernandez Del Olmo, M., Cheeran, B., Ruge, D., Schippling, S., Caltagirone, C., Rothwell, J.C., 2007. Focal stimulation of the posterior parietal cortex increases the excitability of the ipsilateral motor cortex. J Neurosci 27, 6815-6822.

Koch, G., Franca, M., Del Olmo, M.F., Cheeran, B., Milton, R., Alvarez Sauco, M., Rothwell, J.C., 2006. Time course of functional connectivity between dorsal premotor and contralateral motor cortex during movement selection. J Neurosci 26, 7452-7459.

Koch, G., Versace, V., Bonni, S., Lupo, F., Lo Gerfo, E., Oliveri, M., Caltagirone, C., 2010. Resonance of cortico-cortical connections of the motor system with the observation of goal directed grasping movements. Neuropsychologia 48, 3513-3520.

Kurata, K., 2018. Hierarchical Organization Within the Ventral Premotor Cortex of the Macaque Monkey. Neuroscience 382, 127-143.

Kurata, K., Tanji, J., 1986. Premotor cortex neurons in macaques: activity before distal and proximal forelimb movements. J Neurosci 6, 403-411.

Lanz, F., Moret, V., Ambett, R., Cappe, C., Rouiller, E.M., Loquet, G., 2017. Distant heterotopic callosal connections to premotor cortex in non-human primates. Neuroscience 344, 56-66.

Lee, H., Gunraj, C., Chen, R., 2007. The effects of inhibitory and facilitatory intracortical circuits on interhemispheric inhibition in the human motor cortex. J Physiol 580, 1021-1032.

Lu, M.T., Preston, J.B., Strick, P.L., 1994. Interconnections between the prefrontal cortex and the premotor areas in the frontal lobe. J Comp Neurol 341, 375-392.

Luppino, G., Matelli, M., Camarda, R., Rizzolatti, G., 1993. Corticocortical connections of area F3 (SMA-proper) and area F6 (pre-SMA) in the macaque monkey. J Comp Neurol 338, 114-140.

Luppino, G., Rizzolatti, G., 2000. The Organization of the Frontal Motor Cortex. News Physiol Sci 15, 219-224.

Marconi, B., Genovesio, A., Giannetti, S., Molinari, M., Caminiti, R., 2003. Callosal connections of dorso-lateral premotor cortex. European Journal of Neuroscience 18, 775-788.

McGlone, F., Kelly, E.F., Trulsson, M., Francis, S.T., Westling, G., Bowtell, R., 2002. Functional neuroimaging studies of human somatosensory cortex. Behav Brain Res 135, 147-158.

Miller, E.K., 1999. The prefrontal cortex: complex neural properties for complex behavior. Neuron 22, 15-17.

Miller, E.K., 2000. The prefrontal cortex and cognitive control. Nat Rev Neurosci 1, 59-65.

Miller, E.K., Cohen, J.D., 2001. An integrative theory of prefrontal cortex function. Annu Rev Neurosci 24, 167-202.

Mochizuki, H., Huang, Y.Z., Rothwell, J.C., 2004. Interhemispheric interaction between human dorsal premotor and contralateral primary motor cortex. J Physiol 561, 331-338.

Neubert, F.X., Mars, R.B., Buch, E.R., Olivier, E., Rushworth, M.F., 2010. Cortical and subcortical interactions during action reprogramming and their related white matter pathways. Proc Natl Acad Sci U S A 107, 13240-13245.

Ni, Z., Gunraj, C., Nelson, A.J., Yeh, I.J., Castillo, G., Hoque, T., Chen, R., 2009. Two phases of interhemispheric inhibition between motor related cortical areas and the primary motor cortex in human. Cereb Cortex 19, 1654-1665.

O'Shea, J., Sebastian, C., Boorman, E.D., Johansen-Berg, H., Rushworth, M.F., 2007. Functional specificity of human premotor-motor cortical interactions during action selection. Eur J Neurosci 26, 2085-2095.

Ongur, D., Ferry, A.T., Price, J.L., 2003. Architectonic subdivision of the human orbital and medial prefrontal cortex. J Comp Neurol 460, 425-449.

Opitz, A., Legon, W., Rowlands, A., Bickel, W.K., Paulus, W., Tyler, W.J., 2013. Physiological observations validate finite element models for estimating subject-specific electric field distributions induced by transcranial magnetic stimulation of the human motor cortex. Neuroimage 81, 253-264.

Pallud, J., Zanello, M., Kuchcinski, G., Roux, A., Muto, J., Mellerio, C., Dezamis, E., Oppenheim, C., 2018. Individual Variability of the Human Cerebral Cortex Identified Using Intraoperative Mapping. World Neurosurg 109, e313-e317.

Petrides, M., Pandya, D.N., 1999. Dorsolateral prefrontal cortex: comparative cytoarchitectonic analysis in the human and the macaque brain and corticocortical connection patterns. Eur J Neurosci 11, 1011-1036.

Petrides, M., Pandya, D.N., 2002. Comparative cytoarchitectonic analysis of the human and the macaque ventrolateral prefrontal cortex and corticocortical connection patterns in the monkey. Eur J Neurosci 16, 291-310.

Petrides, M., Tomaiuolo, F., Yeterian, E.H., Pandya, D.N., 2012. The prefrontal cortex: comparative architectonic organization in the human and the macaque monkey brains. Cortex 48, 46-57.

Rizzolatti, G., Cattaneo, L., Fabbri-Destro, M., Rozzi, S., 2014. Cortical mechanisms underlying the organization of goal-directed actions and mirror neuron-based action understanding. Physiol Rev 94, 655-706.

Rossini, P.M., Burke, D., Chen, R., Cohen, L.G., Daskalakis, Z., Di Iorio, R., Di Lazzaro, V., Ferreri, F., Fitzgerald, P.B., George, M.S., Hallett, M., Lefaucheur, J.P., Langguth, B., Matsumoto, H.,

Miniussi, C., Nitsche, M.A., Pascual-Leone, A., Paulus, W., Rossi, S., Rothwell, J.C., Siebner, H.R., Ugawa, Y., Walsh, V., Ziemann, U., 2015. Non-invasive electrical and magnetic stimulation of the brain, spinal cord, roots and peripheral nerves: Basic principles and procedures for routine clinical and research application. An updated report from an I.F.C.N. Committee. Clin Neurophysiol 126, 1071-1107.

Rothwell, J.C., Hallett, M., Berardelli, A., Eisen, A., Rossini, P., Paulus, W., 1999. Magnetic stimulation: motor evoked potentials. The International Federation of Clinical Neurophysiology. Electroencephalogr Clin Neurophysiol Suppl 52, 97-103.

Rouiller, E.M., Babalian, A., Kazennikov, O., Moret, V., Yu, X.H., Wiesendanger, M., 1994. Transcallosal connections of the distal forelimb representations of the primary and supplementary motor cortical areas in macaque monkeys. Exp Brain Res 102, 227-243.

Rowe, J., Hughes, L., Eckstein, D., Owen, A.M., 2008. Rule-selection and action-selection have a shared neuroanatomical basis in the human prefrontal and parietal cortex. Cereb Cortex 18, 2275-2285.

Rowe, J.B., Stephan, K.E., Friston, K., Frackowiak, R.S., Passingham, R.E., 2005. The prefrontal cortex shows context-specific changes in effective connectivity to motor or visual cortex during the selection of action or colour. Cereb Cortex 15, 85-95.

Shimazu, H., Maier, M.A., Cerri, G., Kirkwood, P.A., Lemon, R.N., 2004. Macaque ventral premotor cortex exerts powerful facilitation of motor cortex outputs to upper limb motoneurons. J Neurosci 24, 1200-1211.

Tanji, J., Hoshi, E., 2008. Role of the lateral prefrontal cortex in executive behavioral control. Physiol Rev 88, 37-57.

Thielscher, A., Opitz, A., Windhoff, M., 2011. Impact of the gyral geometry on the electric field induced by transcranial magnetic stimulation. Neuroimage 54, 234-243.

Tomassini, V., Jbabdi, S., Klein, J.C., Behrens, T.E., Pozzilli, C., Matthews, P.M., Rushworth, M.F., Johansen-Berg, H., 2007. Diffusion-weighted imaging tractography-based parcellation of the human lateral premotor cortex identifies dorsal and ventral subregions with anatomical and functional specializations. J Neurosci 27, 10259-10269.

Toogood, J.A., Smith, R.C., Stevens, T.K., Gati, J.S., Menon, R.S., Theurer, J., Weisz, S., Affoo, R.H., Martin, R.E., 2017. Swallowing Preparation and Execution: Insights from a Delayed-Response Functional Magnetic Resonance Imaging (fMRI) Study. Dysphagia 32, 526-541.

Vigano, L., Fornia, L., Rossi, M., Howells, H., Leonetti, A., Puglisi, G., Conti Nibali, M., Bellacicca, A., Grimaldi, M., Bello, L., Cerri, G., 2019. Anatomo-functional characterisation of the human "hand-knob": A direct electrophysiological study. Cortex 113, 239-254.

Wise, S.P., Boussaoud, D., Johnson, P.B., Caminiti, R., 1997. Premotor and parietal cortex: corticocortical connectivity and combinatorial computations. Annu Rev Neurosci 20, 25-42.

Wise, S.P., Murray, E.A., Gerfen, C.R., 1996. The frontal cortex-basal ganglia system in primates. Crit Rev Neurobiol 10, 317-356.

Yamagata, T., Nakayama, Y., Tanji, J., Hoshi, E., 2012. Distinct information representation and processing for goal-directed behavior in the dorsolateral and ventrolateral prefrontal cortex and the dorsal premotor cortex. J Neurosci 32, 12934-12949.

Supplementary Materials

Supplementary Methods

Data Analysis

Additional analysis was performed to show that there was significant connectivity between right frontal regions and left M1 for each task. Here, individual T-test maps for rest, Prep-ABD and Prep-PG were created by performing a one-sample T-test at each vertex of the fsaverage template surface for each condition separately. Maps and ROIs were created, which showed vertices that significant t-values ($p<0.05$) and included at least 55 vertices. The centroid of each cluster was identified, and the region labelled by relating it to subdivisions of the cortex based on the Human Connectome Project brain atlas (Glasser et al., 2016). The anatomical subdivisions and centroids for each cluster are shown in Supplementary Figure S2.

Supplementary Results

T-value maps during rest, Prep-ABD and Prep-PG

To further illustrate that there were significant changes in contralateral test MEPs after conditioning right hemisphere TMS, T-test value maps were created for each condition (rest, Prep-ABD, Prep-PG) identified by the one-sample t-test results. Figure S3 shows the one-sample t-test motor maps where significant vertices were thresholded at $p<0.05$ and clusters identified to show significant facilitation (red) or inhibition (blue) of conditioned MEPs. In line with the One-way ANOVA results (Fig. 3), at rest, clusters in area 6v, 43 and 44 (Fig. S2; Table S1) showed significant facilitation of contralateral conditioned MEPs ($p<0.05$; Fig. S3A, D, G). In addition to these regions, area 6d/FEF, area 45 and 8Av (Fig. S2; Table S1) also showed significant facilitation of contralateral conditioned MEPs ($p<0.05$; Fig. S3A, D, G; Table S1). During Prep-ABD, a cluster in area 8C (Fig. S2; Table S1) showed similar inhibition of contralateral conditioned MEPs as in the main results ($p<0.05$; Fig. S3B, E, H). An additional cluster in area IFSa, which overlaps with area 45, also showed significant inhibition of contralateral conditioned MEPs ($p<0.05$; Fig. S3B, E, H). As in the main results, during Prep-PG, a large cluster with its centroid in IFSp but overlaps area 44 (Fig. S2; Fig. S3I; Table S1) showed significant facilitation of contralateral MEP size ($p<0.05$; Fig. S3C, F, I). While a cluster in premotor region area 6r overlapping with 6v resulted in significant inhibition, a cluster in area 6d/FEF resulted in the facilitation of contralateral conditioned MEPs during Prep-PG

(p<0.05; Fig. S3C, F, I). Finally, similar to previous one-way ANOVA results (Fig. 3C), significant clusters found in DLPFC region area 46 and 8Av resulted in the facilitation of the contralateral conditioned MEPs during Prep-PG (p<0.05; Fig. S3C, F, I). Additionally, a cluster in area p9-46v also showed facilitation of the contralateral conditioned MEPs (p<0.05; Fig. S3C, F, I).

Supplementary Figures

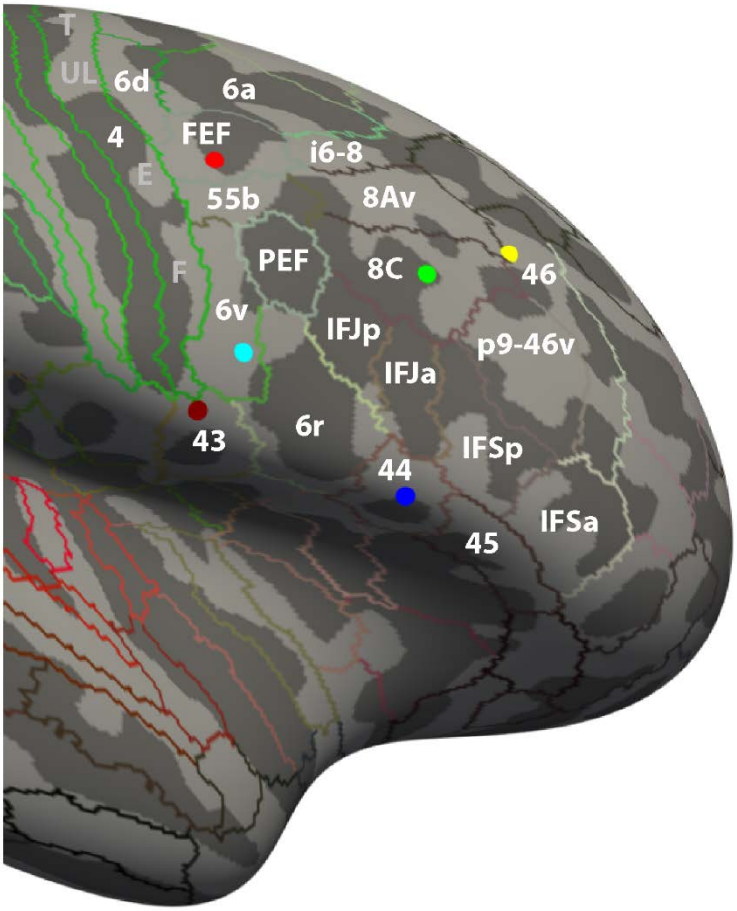

Figure S1. One-way ANOVA cluster centroids. *The Human Connectome Project brain atlas (Glasser et al., 2016) was mapped onto the Freesurfer average brain to identify subdivisions of the frontal cortex. The cluster centroids were plotted on the Freesurfer using MNI coordinates; red – area 6d/frontal eye fields (FEF), cyan - area 6v, dark red - area 43, blue - area 44, green - area 8C, yellow – 8Av (border with area 46 and 8C).*

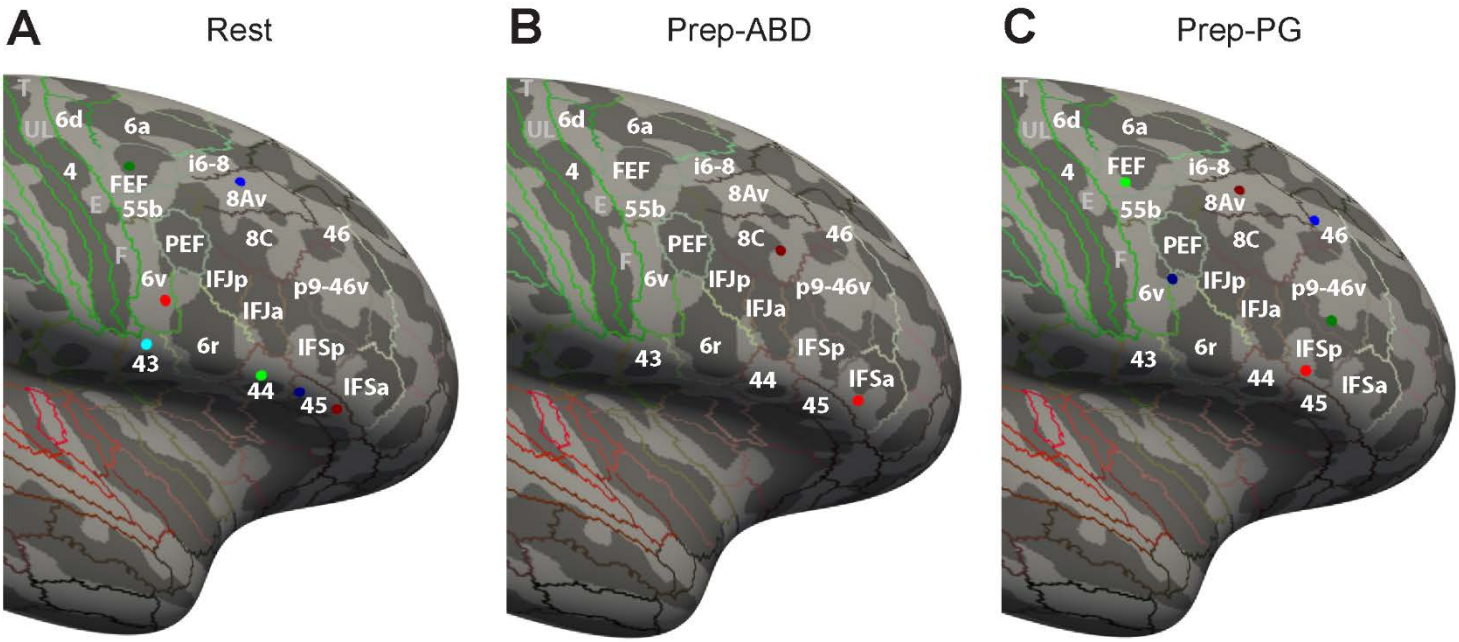

Figure S2. T-test cluster centroids. *The Human Connectome Project brain atlas (Glasser et al., 2016) was mapped onto the Freesurfer average brain to identify subdivisions of the frontal cortex. The cluster centroids were plotted on the Freesurfer using MNI coordinates;* ***A****. Rest: red - area 6v, cyan - area 43, dark red - area 45, blue - area 45, green - area 44, dark blue – area 8Av.* ***B.*** *Prep-ABD: red – area IFSa, dark red – area 8C.* ***C.*** *Prep-PG: red - area IFSp, dark red - area 8Av, blue - area 46, dark blue – area 6r, green – area 6d/FEF, dark green – p9-46v*

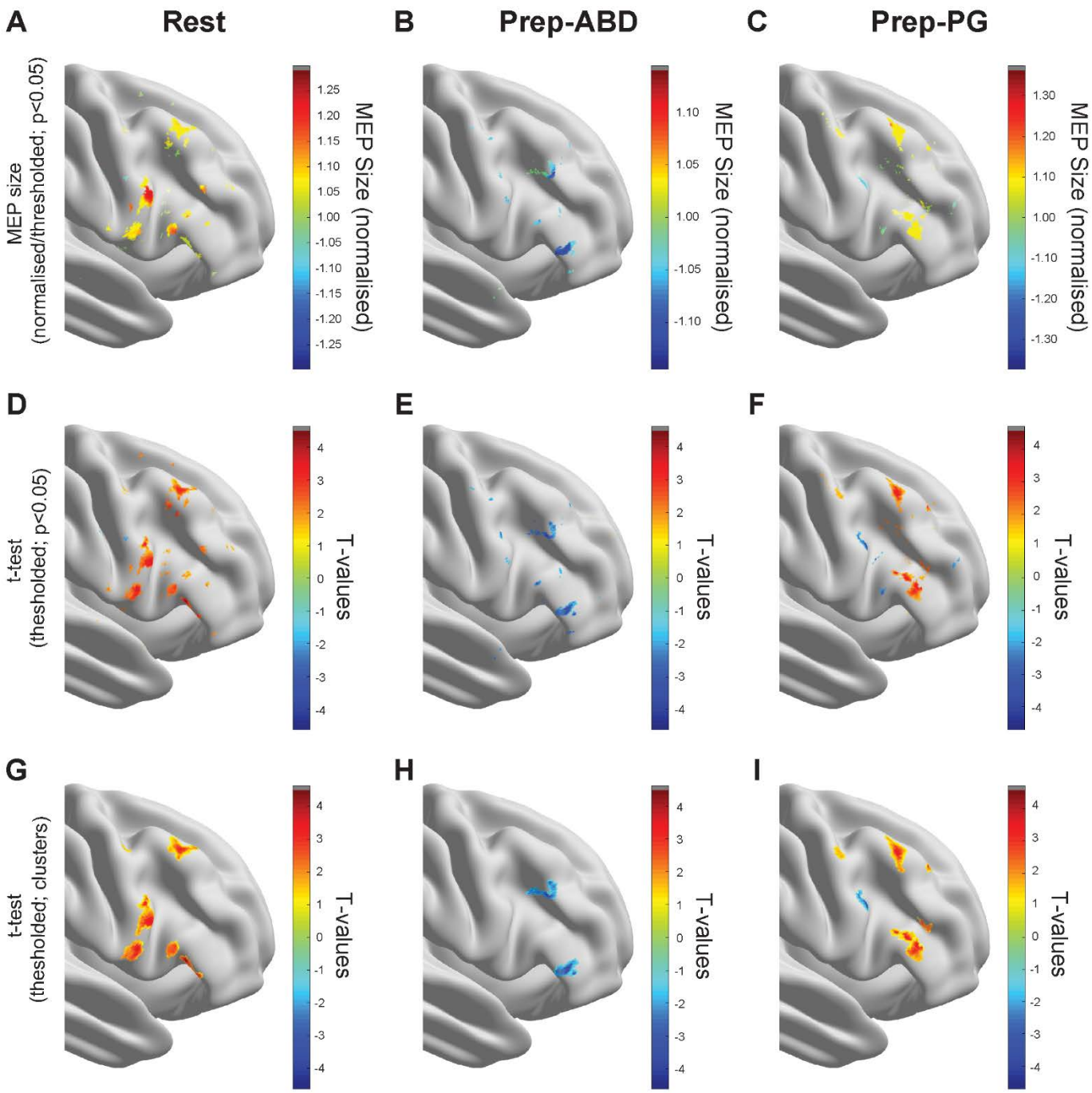

Figure S3. MEP and T-test thresholded motor maps. *MEP and T-value motor maps during rest (A), Prep-ABD (B) and Prep-PG (C), where T-values were thresholded at p<0.05 creating sub-clusters in the frontal cortex region for MEP size and T-values. MEP size colour scale represents normalised MEP size; where blue represents inhibition (less than 1) of the contralateral MEPs after conditioning right hemisphere TMS and red represents facilitation (greater than 1) of the contralateral MEPs after conditioning right hemisphere TMS. T-test value colour scale represents T-values; where blue represents positive T-values and red represents negative T-values.*

Tables

Table S1. Rest T-value maps: Corresponding brain anatomy, brain area (Glasser et al., 2016), active cluster size (total no. of vertices) and MNI coordinates

Neuroanatomy	**Area**	**Cluster Size**	**X**	**Y**	**Z**
Dorsal precentral gyrus	6d/FEF	65	42.12	-3.70	47.34
Ventral precentral gyrus	6v	260	56.32	7.54	29.30
Ventral precentral gyrus	43	159	62.60	2.41	13.75
Middle frontal gyrus	8Av	162	39.60	22.63	7.40
Inferior frontal gyrus – Pars opercularis	44	69	57.95	16.55	14.93
Inferior frontal gyrus – Pars triangularis	45	90	55.12	22.63	7.40
Inferior frontal gyrus – Pars triangularis	45	56	54.06	27.16	1.60

Table S2. Prep-ABD T-value maps: Corresponding brain anatomy, brain area (Glasser et al., 2016), active cluster size (total no. of vertices) and MNI coordinates

Neuroanatomy	**Area**	**Cluster Size**	**X**	**Y**	**Z**
Middle frontal gyrus	8C	220	41.36	19.44	33.23
Inferior frontal gyrus	IFSa	172	53.34	31.93	4.09

Table S3. Prep-PG T-value maps: Corresponding brain anatomy, brain area (Glasser et al., 2016), active cluster size (total no. of vertices) and MNI coordinates

Neuroanatomy	**Area**	**Cluster Size**	**X**	**Y**	**Z**
Dorsal precentral gyrus	6d/FEF	76	46.92	-2.46	51.15
Ventral precentral gyrus	6r	138	49.47	5.35	32.82
Middle frontal gyrus	8Av	151	41.41	20.20	48.45
Middle frontal gyrus	p9-46v	102	44.33	29.85	20.30
Middle frontal gyrus	46	58	33.39	31.67	40.99
Inferior frontal gyrus	IFSp	251	54.06	27.16	1.60